RSC Advances

PAPER

View Article Online
View Journal | View Issue

Cite this: *RSC Adv.*, 2025, **15**, 35022

Long-acting injectable nanoemulsion for anti-inflammatory therapy: luteolin and resveratrol-loaded CMC formulation regulates TH1/TH2 homeostasis in ovalbumin-induced allergic rhinitis in mice models

Pei Lin, *[a] Gowripriya Thirumugam,[b] Thiyagarajan Manickam,[c] Govindaraj Dharman[d] and Kalaiyarasi Jayaprakasam[e]

Allergic rhinitis (AR) continues to be a substantial global health concern, requiring the development of effective treatment methods. With an aim of enhancing medicine administration for the treatment of allergic rhinitis, the present work investigates the synthesis and characterization of a nanoemulsion consisting of luteolin (LTN) and resveratrol (RSV) encapsulated in carboxymethyl chitosan (CMC). Unlike traditional oral drugs, this formulation, upon nasal administration, avoids first-pass metabolism and achieves faster and stronger action. At various feed concentrations, LTN's and RSV's loading capacity was assessed to show optimal absorbance, mass of drug loading, and encapsulating efficiency. By means of their zeta potentials, particle size measurements indicated hydrated particle diameters of 215.3 ± 0.1 nm for LTN and 123.63 ± 0.1 nm for RSV, indicating appropriate stability. Functional groups and crystallinity in the formulations were confirmed by FTIR spectroscopy and X-ray diffraction. TEM and SEM morphological studies revealed spherical nanoemulsion droplets showing minimal aggregation. The highest encapsulation efficiencies were LTN at 96.75% and RSV at 97%. *In vitro* release experiments on the nanoemulsions showed far higher drug release rates compared with the raw materials. Based on biocompatibility testing, LTN/RSV@CMC exhibited minimal cytotoxicity and hemolysis rates of less than 5%. *In vivo* experiments using a mouse model of AR showed that administration of LTN/RSV@CMC substantially lowered allergy symptoms, histamine levels, cytokine production, and inflammatory cell-infiltration in NLF. The results reveal that LTN/RSV@CMC is a suitable therapeutic agent for AR, suppresses inflammatory responses, and has excellent safety characteristics.

Received 3rd May 2025
Accepted 19th August 2025

DOI: 10.1039/d5ra03121d

rsc.li/rsc-advances

1. Introduction

The primary cause of allergic rhinitis (AR), a chronic inflammatory illness of the nasal mucosa, is immunoglobulin E (IgE) produced in reaction to allergens, especially in people with atopic disorders. The quality of life of affected people is considerably reduced by the disorder, which is characterized by symptoms including recurrent nasal itching, sneezing, rhinorrhea, and nasal blockage.[1] Furthermore, AR imposes a substantial economic burden on society because to healthcare costs and lost productivity.[2] About forty percent of the global population is affected by AR; incidence among children has increased significantly.[3] Influenced by Th2 cells, AR, a classic immune-mediated disorder, is typified by ongoing inflammatory reactions that call for efficient treatment plans.[4]

Particularly in the activation of T cells and boosting B cell survival, cytokines are very important in inflammatory reactions linked with AR.[5] Pyroptosis, a kind of programmed cell death involved in AR pathogenesis, is linked to the NLR family pyrin domain containing 3 (NRRP3) inflammasome.[6] By increasing inflammatory responses and epithelial pyroptosis, the activation of NLRP3 inflammasomes increases AR, thereby causing more tissue damage and inflammation.[7] Previous research has shown that the nasal mucosa of AR patients show higher levels of proinflammatory cytokines, including TNF-α, IL-1, and IL-8, thereby suggesting their major importance in mediating allergic inflammation.[8] These cytokines help recruit and activate a range of immune cells, thereby contributing to the

[a]*Department of Otolaryngology Head and Neck Surgery, Shaanxi Provincial People's Hospital, Xi'an-710086, China. E-mail: linp5505@sina.com; Tel: +86 15686455505*
[b]*Centre for Pharmacology & Toxicology Research, Sciliv PVT LTD, Dharmapuri, Tamil Nadu-636801, India*
[c]*Centre for Cell and Molecular Biology, Sciliv PVT LTD, Dharmapuri, Tamil Nadu-636801, India*
[d]*Centre for Nanobiomedicine, Sciliv PVT LTD, Dharmapuri, Tamil Nadu-636801, India*
[e]*Centre for Bioanalytical Research, Sciliv PVT LTD, Dharmapuri, Tamil Nadu-636801, India*

continuation of symptoms.[9] As a crucial component of the innate immune system, macrophages engage with allergens at the first stages of the immune response.[10] Recent studies on the innate immune system show that *via* generation of cytokines and inflammatory lipid mediators,[11] macrophages greatly affect both innate and adaptive immune responses. As essential components of the immune response in the nasal mucosa, nasal macrophages help to maintain immunological homeostasis.[12]

Pattern recognition receptors (PRRs)[13] recognize several allergens and pathogens that the airways are constantly exposed to. Of them, the NLRP3 is identified as a fundamental element of the pyroptotic signalling pathway.[14] Functioning as the effector protein, the NLRP3 inflammasome consists of caspase-1, the adaptor-protein (Pycard), and NLRP3 receptor.[15] Research shows that allergens can set up the NLRP3 inflammasome, therefore encouraging type 2 immune responses and aggravating allergic inflammation.[16] Managing AR successfully depends on striking a balance between these competing factors.[17] Immune cells and cytokines engage in intricate interactions within pathophysiology, resulting in both immediate and delayed hypersensitivity responses.[18] The prevention and treatment of AR depend on the reduction of the excessive activation of localized inflammatory responses in the nose mucus membrane.[19] Given the increasing frequency of this prevalent disease and associated complications, improved therapy approaches are absolutely needed to appropriately control it.[20]

Western healthcare offers leukotriene receptor antagonists, glucocorticoids, anti-IgE biological substances, anti-IgE biological agents, mast cell stabilizing agents, and allergy medications. Although they offer the rapid relief of symptoms, these drugs have limitations in clinical use, including possible adverse effects and the possibility of symptom reappearance upon treatment cessation.[21] Earlier studies on nanoparticle-based AR are increasingly attracting more attention considering these difficulties.[22] These recently developed treatments aim to improve drug distribution and efficacy, and reduce side effects.[23] Targeting damaged sections of the nasal mucosa, nanoparticles help therapeutic medications be more absorbed.[24]

Luteolin (LTN), a natural flavonoid that is found in a variety of plants, including fruits, vegetables, and medicinal botanicals, is frequently referred to as 3′,4′,5,7-tetrahydroxyflavone.[25] Since antiquity, LTN, known for its distinctive yellow crystalline form—has been used as a dye largely from the plant *Reseda luteola*.[26] Among the several biological activities of LTN, some noteworthy ones include antioxidant, anti-inflammatory, and anticancer properties.[27] Luteolin effectively reduces oxidative stress and eliminates reactive oxygen species, therefore protecting cells from damage.[28] Its anti-inflammatory qualities are ascribed to its power to control inflammatory pathways by reducing pro-inflammatory cytokines such as TNF-α, IL-1β, and -6, in addition to interfering with vital paths such as MAPK and NF-κB.[29] Inspired by its immunomodulating qualities, LTN has been put forth as a potential treatment for allergic asthma and rhinitis.[30] Studies of allergic animal models reveal that it can lower bronchoconstriction and airway hyper responsibility.[31] In mouse allergic asthma and rhinitis, a research study found that LTN drastically reduced cellular intrusion in the nasal and pulmonary tissues.[32] It has also proved successful in lowering excess mucus output in allergy murine models and suppressing airway inflammation in asthmatic rat models.[33] Despite these encouraging results, the precise mechanisms regulating LTN's immunomodulating activity remain unknown.[34] Previous research suggests that its anti-allergic properties may be derived from its capacity to inhibit mast cell activation and modify proteins associated with inflammation.[35] Despite this, there is still a lack of sufficient research on the impact of LTN on type 2 helper T (TH2) cells, which underscores a potential area for future research.[36]

Resveratrol (RSV), commonly called as *trans*-3,5,4′-trihydroxystilbene,[37] is a prominent polyphenol primarily found in grapes, berries, peanuts, and other plants. Particularly with respect to cardiovascular health, anti-inflammatory properties, and cancer prevention, RSV has drawn attention for its putative advantages for health.[38] RSV acts as an antioxidant by neutralizing dangerous free radicals and therefore lowering oxidative stress connected with chronic diseases.[39] By suppressing cyclooxygenase (COX-1 and -2) enzymes and thereby altering important cellular pathways linked to many disorders, including NF-κB, Wnt, and PI3K/Akt/mTOR, it also reduces inflammation. Moreover, resveratrol mimics the effects of calorie restriction, hence possibly extending lifespan and enhancing metabolic health. Resveratrol has been shown in studies to reduce mast cell activation, hence lowering allergy symptoms.[40,41] In allergic situations, animal trials show promise in reducing bronchoconstriction and airway hyper responsibility.[42]

Toxicity from metal oxides, nanoparticles agglomeration, and immune response are key important considerations in drug delivery. To overcome these issues, natural polymers with a non-toxic, biocompatible, biodegradable and non-immunogenic nature are great building blocks for creating nanocarriers and functionalizing drug delivery system (DDS) surfaces. Chitosan (CS) is a linear polysaccharide made up of *N*-acetyl-D-glucosamine (acetylated) and beta-(1–4)-linked D-glucosamine (deacetylated) that are dispersed at random. Notably, CS demonstrates strong mucoadhesion (mucous membranes), which are advantages for nasal delivery and sustained local drug retention in allergic rhinitis treatment.[43] Although CS is soluble at acidic pH levels, its insolubility in water is a disadvantage for employment in biomedical applications. For allergic rhinitis, modified CS, such as quaternized chitosan and *N*-carboxyethyl CS (NCS) shows enhanced water solubility, a broader pH solubility. These changes encourage cell proliferation and mucosal adhesion, and enable sequential or prolonged drug release. This can lead to improved symptom control for allergic rhinitis, decreased dosing frequency, decreased IgE and cytokine levels, and long-lasting anti-inflammatory effects.[44]

This investigation provides a novel method for the management of AR by co-loading LTN and RSV into a nanoemulsion that is intended for nasal administration. This

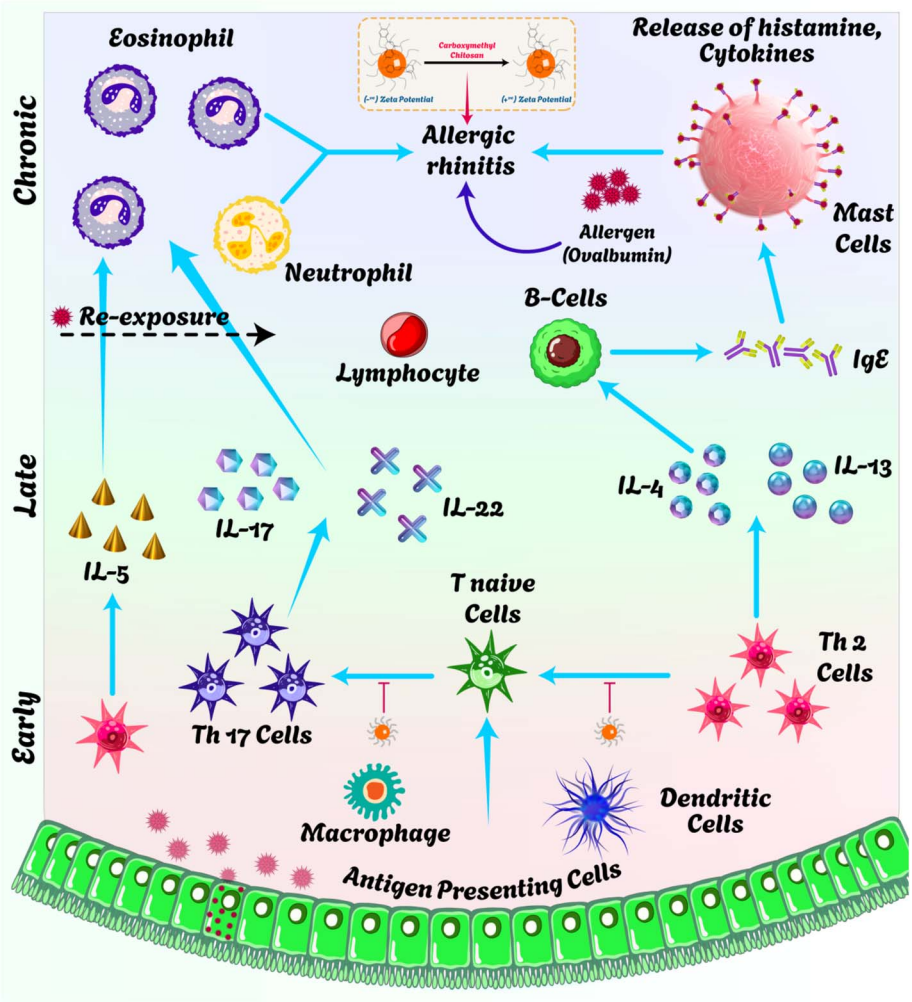

Fig. 1 Schematic representation of immune modulation in the AR model treated with LTN/RSV@CMC.

approach aims to maximize the therapeutic efficacy of these molecules by lowering their systemic side effects usually connected with conventional oral drugs and raising their bioavailability. Emphasizing important properties including loading capacity, particle size, zeta potential, and encapsulation efficiency, a complete *in vitro* evaluation of the formulation was conducted. With great safety profiles and effective modulation of inflammatory responses, the study finds LTN/RSV@CMC to be a potential AR treatment candidate (Fig. 1).

2. Materials and methods

2.1 Synthesis and analysis of LTN/RSV@CMC

To formulate the LTN/RSV@CMC nanoemulsion, two distinct oil phases were initially prepared: one by sonicating 10 mg of LTN in 1 mL of PEG-400, and the other by sonicating 50 mg of RSV in 1 mL of PEG-400 for 5 minutes each at ambient temperature to achieve homogeneous solutions. Subsequently, the two oil phases are combined and introduced dropwise into 50 mL of an aqueous CMC solution, while maintaining continuous magnetic stirring at ambient temperature. This procedure generates the preliminary nanoemulsion. To improve particle stability and dispersion, 10 mg of sodium tripolyphosphate (TPP) is incorporated as a cross-linking agent into the mixture and stirred continuously. The ionic gelation method was used to formulate the LTN/RSV@CMC nanoemulsion. The negatively charged sodium tripolyphosphate ions engage with the positively charged amino groups of the CMC, resulting in the cross-linking of polymer chains (ionic gelatin). Subsequently, the entire solution is transferred to a Teflon flask and lyophilized for 6 hours at −40 °C to yield the final product, the LTN/RSV@CMC nanoemulsion. The resultant product must be enclosed in a Ziploc bag and refrigerated at 5 °C until it is prepared for subsequent physicochemical and biological analyses.

2.2 Particle size and zeta potential analysis

The parameters of the LTN/RSV@CMC formulation were investigated using particle size and zeta potential measurements. In the hydrated complex, the mean distance between water molecules and ions is expressed by the particle size; smaller values indicate a more compact structure. The measure

of the degree of stability of the particulate system is the charge on particle surfaces, sometimes known as the zeta potential or surface potential. For the aim of the zeta potential and particle size analysis, a Zetasizer Nano's sample chamber held roughly 0.2–1.0 mL of LTN/RSV@CMC. The temperature was kept at 25 °C and the sample concentration was decided upon as one milligram per millilitres. Three measurements for every parameter helped to precisely evaluate the hydrated particle size and zeta potential of LTN/RSV@CMC.

2.3 Appearance, viscosity and pH

The developed LTN/RSV@CMC nanoemulsions were visually assessed for transparency by means of light reflections, therefore enabling clear determination. Using a constant temperature of 25 °C, the acidity or alkalinity of the nanoemulsions was ascertained using a pH meter (Omega). To precisely evaluate the flow properties of the emulsion, viscosity was measured with a Brookfield viscometer (LVF 697) under a UL-adapter. With the temperature maintained at 25 °C throughout the studies, all tests were carried out three times to guarantee consistent and dependable data.

2.4 Functional characterization of LTN/RSV@CMC

2.4.1 FTIR. The Fourier transform infrared (FTIR) spectra of LTN, RSV, CMC and LTN/RSV@CMC combination were examined utilizing a PerkinElmer FTIR spectrometer. Disks of potassium bromide were formed by crushing samples (5 mg). The spectra were acquired within a wavenumber range of 500 to 4000 cm^{-1}.

2.4.2 X-ray diffraction analysis. The crystallinity of LTN/RSV@CMC in the cross-linked nanoemulsion was examined using an XRD (ULTIMA-III, Japan). This investigation employed nickel-filtered Cu Kα-radiation at 35 kV and 25 mA for both the pure medication and the formed microparticles.

2.5 Morphological analysis

2.5.1 TEM. The morphology of LTN/RSV@CMC was examined utilizing a transmission electron microscope (JEM2100, Japan). The nanoemulsion was diluted with water that had been deionized and applied to a copper mesh for analysis. To improve image quality, a 2% w/v solution of phosphotungstic acid was utilized as a negative stain, adhering to a previously published protocol.[45]

2.5.2 SEM. The structure of the LTN/RSV@CMC nanoemulsion was additionally verified using a scanning electron microscope (SEM). This procedure involved the positioning of samples on a polycarbonate substrate, the elimination of surplus water through air-drying at room temperature, and the utilization of CO_2. Next, the samples were coated with gold to improve conductivity before examination with a SEM (JEOL Datum Ltd, Tokyo, Japan), operating at 20 kV.

2.6 *In vitro* drug release study

The dialysis bag technique was employed to assess the *in vitro* dispersal efficacy of the system for drug delivery,[46] wherein a 5 mg sample of LTN/RSV@CMC powder was solubilized in 1.5 mL of phosphate-buffered saline (PBS) at pH 7.4 and subsequently positioned within a dialysis membrane bag with a molecular weight cutoff of 12 kDa. The bag was thereafter submerged in a beaker with 50 mL of PBS, calibrated to replicate a nasal pH of 6.5, and agitated continuously at 37 °C at 100 rpm. Subsequently, 1.5 mL samples were extracted from the beaker and replaced with fresh PBS to maintain consistent conditions at the scheduled intervals (0, 1, 2, 3, 4, 5, 6, 7 and 8 hours). The absorbance of these samples was assessed at 370 nm to quantify the released LTN and RSV, utilizing a standard curve for measurement. Each experiment was performed in triplicate to assure precision, and the cumulative release rate of LTN and RSV was determined.

2.7 *In vitro* cytotoxicity analysis

2.7.1 Cell culture. NIH/3T3 cells were procured from the Cell Bank of the Chinese Academy of Sciences in Shanghai, China. NIH-3T3 cells were cultivated in Dulbecco's modified Eagle's medium (DMEM) supplemented with 10% fetal bovine serum (FBS, Gibco, Brooklyn, NY, USA) and maintained at 5% CO_2 and 37 °C.

2.7.2 Cell viability analysis. Cellular viability was investigated using the Cell Counting Kit-8 (CCK-8) test on the LTN/RSV@CMC nanoemulsion. NIH 3T3 cells were planted in a 96-well plate, and then treated for 12 hours to improve cell adherence. After that, the cells underwent different dosages of LTN/RSV@CMC for the specified times. After the treatment, each well received 100 μL of a 10% concentration of CCK-8 and underwent two more hours of cell culture. Every well's absorbance at 450 nm was measured on a microplate reader. By means of a comparison of absorbance values with those of the control group, the cytotoxic effects of the LTN/RSV@CMC nanoemulsion were quantitatively assessed on NIH 3T3 cells, therefore enabling the evaluation of cell viability.

2.7.3 Live/dead staining. Cell viability was evaluated using a live/dead staining technique combining propidium iodide (PI) with acridine orange (AO). NIH 3T3 cells were grown in plates with 96 wells at a cell density of 4.5×10^5 cells per mL with varied concentrations of LTN/RSV@CMC over 12, 24, and 48 hours. For five minutes in darkness, the cells were subjected to a 1 : 1 mixture of AO and PI. The cells were examined with a fluorescence microscope after rinsing under PBS. Nonviable and viable cells display correspondingly green and red fluorescence, respectively.

2.7.4 Immunofluorescence assay. NIH 3T3 cells were cultured on coverslips with the LTN/RSV@CMC nanoemulsion and subsequently fixed with paraformaldehyde (4%) in PBS for 15 min. Subsequently, the cells were treated with 45 mM NH_4Cl, permeabilized with 0.25% Triton (X-100), and blocked with 0.25% pig skin gelatin (Sigma Aldrich). The antibodies were purchased from Sino Biological, Beijing, China. The cells were subsequently treated with primary antibodies for 2 hours at ambient temperature, washed thrice with PBS, and subsequently incubated with secondary antibodies conjugated to a fluorophore for an additional 2 h at room temperature.

Following washing, the samples were mounted on slides using Aqua-Poly/Mount (Polysciences) and examined with a Zeiss LSM510 META/FCS confocal laser scanning microscope. Nuclear DNA was stained with Draq5 (BioStatus).

2.7.5 Cell migration analysis. NIH-3T3 cells were inoculated in a 6-well tissue culture plate with an initial density of 2.5 $\times$ 10^5 cells per cm^2 and left to incubate overnight. A scrape wound was introduced in the cell monolayer using a micropipette tip. The cells were next treated in DMEM supplemented with 5% FBS using LTN/RSV@CMC. Baseline images of the afflicted areas were obtained; later images were collected two, four-, and six-hours following incubation.

2.8 *In vivo* analysis

2.8.1 Ethical approval. All animal procedures were performed in accordance with the Guidelines for the Care and Use of Laboratory Animals of Shaanxi Provincial People's Hospital. The institutional Animal Ethics Committee provided approval for the investigation (approval no. A2024000710). All experimental procedures were implemented in compliance with the ARRIVE guidelines (*PLoS Biol.*, 2010, **8**(6), e1000412)[47] and pertinent institutional and national regulations. Mice were euthanized with carbon dioxide in strict adherence to the AVMA Guidelines for the Euthanasia of Animals (2020)[48] and the "Guidelines for the Euthanasia of Experimental Animals" (GB/T 39760-2021) in this investigation. Additionally, every effort was made to mitigate pain and distress.

2.8.2 AR mouse model with OVA. Mice were acquired from Jiangsu Huachuang Xinnuo Pharmaceutical Technology Co., Ltd (Jiangsu, China). The animals were maintained in a controlled laboratory environment with a temperature range of 20–26 °C (with a daily variation of $\leq$4 °C) and a humidity range of 40–70%. A 12-hour light/dark cycle was maintained, and the rodents were provided with water and a pelleted commercial diet on an ad libitum basis.

The mice were assigned at random to five groups. In the AR group, on days 0, 6, 12, and 21, the mice were sensitized through intraperitoneal injection with 400 μg of ovalbumin (OVA, Sigma, St. Louis, MO, USA) and 2 mg of aluminum hydroxide (Sigma) dissolved in 200 μL of PBS, followed by nasal cavity injections of 400 μg OVA in 20 μL PBS on days 7, 14, and 21. The control group adhered to the same schedule, but was administered PBS instead of OVA. Subsequently, the confirmed AR mice received a food enriched with RSV (50 mg kg^{-1}) and LTN (10 mg kg^{-1}) at different dosages daily from day 1 to day 21. The mice were euthanized on day 21 for subsequent study.

2.8.3 Allergic score, nasal sneezing, and rubbing. The severity of allergic rhinitis was assessed based on common symptoms like nose irritation, sneezing, nasal discharge, conjunctivitis, and eye discharge. Symptoms were rated on a scale from 0 to 3 to establish a scoring system for classification. Nasal irritation was assigned scores as follows: 0 = no nose rubbing; 1 = 1–2 nose rubs per minute; 2 = 4–6 nose rubs per minute; 3 = more than 6 nose rubs per minute. Sneezing was quantified as follows: 0 = none; 1 = 1–3 sneezes within 10 minutes; 2 = 4–9 sneezes within 10 minutes; and 3 = more than 10 sneezes within 10 minutes. Nasal mucus was assessed using the following scores: 0 = no mucus; 1 = mucus present within a nostril; 2 = mucous outside a nostril; and 3 = excessive mucus overflow. Eye secretions were categorized as follows: 0 = absent; 1 = present within the eye; 2 = present outside the eye; and 3 = excessive or altered in color. Conjunctivitis rating was as follows: 0 = none; 1 = mild; 2 = moderate; 3 = severe. On the initial day following sensitization, primary symptoms including nose sneezing, nasal discharge and rubbing were documented to create a baseline before the commencement of treatment. The allergic rhinitis model's effectiveness was determined by a symptom score above seven, while treatment success required a score below four.[49]

2.8.4 Toxicity assessment. To assess the toxicity levels of the supplied medicines, the body weights of the mice were documented prior to euthanasia. This data enabled a comparison analysis among the several groups, permitting an evaluation of the therapies' effects on the overall body weight in the mice. Through the examination of these weight fluctuations, we sought to get initial insights into the possible toxicity levels linked to each pharmacological intervention.

2.8.5 Real-time PCR analysis. The Hi-cDNA Synthesis Kit (Takara Bio, USA) was employed to synthesize cDNA from identical quantities of total RNA in each sample. Real-time PCR was performed using TNF-α, IL-4, -10, -5, -13, -17, exotoxin and IFN-γ. PCR was done using SYBR Green dye and the Quant-Studio 5 Real-Time PCR machine. The threshold cycle (Ct) method was employed to quantify the relative concentrations of the substances. The relative expression was calculated using the method $2^{(-\Delta\Delta Ct)}$.

2.8.6 Measurement of parameters of inflammation. To assess the efficacy of LTN/RSV@CMC, we quantified different inflammatory markers before and following therapy, including serum-specific IgE, IL-17, TNF-α, and IL-4. Serum-specific IgE functions as a marker for immediate-type allergic reactions, including AR. IL-17 is crucial for regulating inflammatory processes by modulating the pro-inflammatory genes regulation in non-hematopoietic cells. TNF-α, or cachectin, is a multifunctional cytokine essential for inflammation, apoptosis, and immune system maturation; it activates the Th17 cellular pathway by interacting with dendritic and tissue cells to produce IL-12 and IL-23, facilitating the differentiation of T cells into Th17 cells that secrete additional cytokines, including IL-17A and IL-6. Simultaneously, IL-4, produced by antigen-presenting cells (APCs), influences the differentiation of $CD4^+$ T cells into effector Th1 or Th2 cells, promoting a Th1/Th2 imbalance in favour of Th2 by augmenting IL-4 production and inhibiting IFN-γ synthesis.

2.8.7 Enzyme-linked immunosorbent assay (ELISA). The concentrations of several cytokines, including IgE, ovalbumin (OVA)-specific IgE, IL-4, -5, -10, -13, and IFN-γ, were measured using Elabscience Biotechnology (China) ELISA kits, adhering to the manufacturer's guidelines. A microplate reader was employed to quantify absorbance at 450 nm. The generation of a standard curve facilitated the determination of the concentration of each sample based on its absorbance values.

2.8.8 Hemolysis test. Blood samples were incubated at 37 °C/60 minutes with PBS (negative control) and distilled water (positive control) and different doses of the LTN/RSV@CMC nanoemulsion. The samples were centrifuged after incubation, and the absorbance of the supernatant in all groups was measured at 540 nm. The hemolysis percentage (%) was subsequently computed using the following formula:

$$\text{Hemolysis (\%)} = [(OD_x - OD_0)/(OD_y - OD_0)] \times 100$$

OD_0, OD_x, and OD_y denote the absorbance values of the diluted blood in the negative control tubes LTN/RSV@CMC nanoemulsion, and diluted blood in the positive control, respectively. The absorbance values of the negative control had been less than 0.03, while those of the positive control tubes ranged from 0.6 to 1.1.

2.8.9 Identification of inflammatory cells. Nasal lavage fluid (NLF) was collected from each group and subsequently diluted with 1 mL of PBS. A hemocytometer (Mindray 3000, China) was employed to evaluate the total leukocyte count. Neutrophils, lymphocytes, and eosinophils were identified and quantified using Wright's–Giemsa staining.

2.8.10 Hematoxylin–eosin (HE) histology analysis. Following the collection of nasal-associated lymphoid tissue (NALF), the mice heads were preserved in a 10% neutral buffered formaldehyde solution (Sigma-Aldrich, USA) for two days. The specimens were then decalcified in 0.1 M EDTA buffer (Bio-solution, Korea) for one month prior to paraffin embedding. Through a coronal cut, the paraffin blocks were separated into 5 μm pieces. Hematoxylin and eosin (HE) were subsequently employed to stain the tissue sections. This histological processing enabled a thorough evaluation of the immune responses in the nasal cavity.

2.8.11 Statistical analysis. Data from three independent investigations were subjected to statistical analysis. The results are presented as the average ± standard deviation (SD) or standard error of the mean (SEM), as appropriate. The Student's *t*-test or repeated measures analysis of variance (ANOVA) were employed to conduct statistical comparisons between groups, depending on the experimental design. The analyses were conducted using the GraphPad Prism software (version 8, San Diego, CA, USA). The statistical significance threshold was defined at $p < 0.05$. The asterisks in the figures indicate specific p-values: *$p < 0.05$, **$p < 0.01$, ***$p < 0.001$, and ****$p < 0.0001$.

3. Results and discussion

3.1 Analysis of LTN and RSV loading capacity in CMC

To find the optimal dosage, the study looked at the effects of LTN and RSV mixed in CMC at varying feed concentrations—

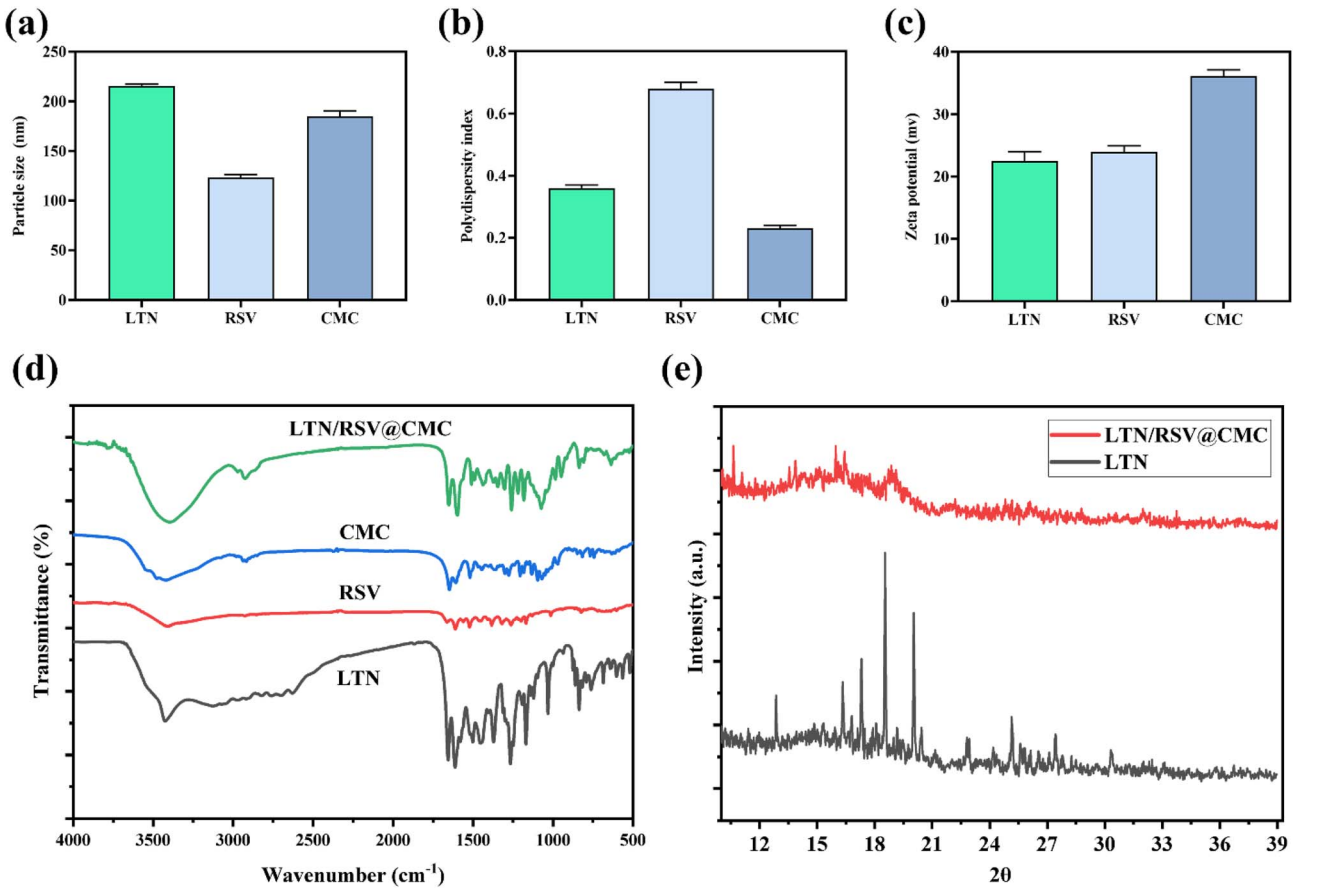

Fig. 2 Characterization of LTN/RSV@CMC nanoemulsion. (a) Particle size, (b) PDI and (c) zeta potential, (d) FTIR pattern, and (e) XRD-pattern.

that is, pure LTN (10 mg kg^{-1}) and RSV (50 mg kg^{-1}). Assessed across the five groups were fundamental parameters, including LTN/RSV@CMC absorbance, drug loading mass, volume, drug loading capacity, encapsulation efficiency, and particle mass.

3.2 Particle size and zeta potential determination

The size of droplets is a vital parameter for evaluating the stability of nano-emulsions and improving drug bioavailability.[50] It profoundly influences medication release and biological absorption. The results showed that the LTN and RSV had particle sizes of 215.3 ± 0.1 nm and 123.63 ± 0.1 nm, respectively. These particles exhibited a uniform particle size distribution with a PDI of 0.359 and 0.679, as well as a zeta potential of 22.5 ± 0.1 mV and 23.8 ± 0.1 mV, which indicated good stability. The particle size of the CMC raw material was 185.8 ± 0.2 nm, with a PDI of 0.219 and a zeta potential of 35.2 ± 0.1 mV. The LTN/RSV@CMC exhibited a higher frequency of particle dispersion over the 200–1400 nm range in comparison to the CMC raw material and a reduced zeta potential, indicating enhanced aggregation (Fig. 2a–c). The LTN/RSV@CMC is optically translucent and has a clearer appearance than other nano-emulsion systems due to its smaller droplet size, which reduces light scattering.[51] These results have demonstrated that the LTN/RSV@CMC nanoemulsions with a high zeta potential exhibit increased stability as a result of their capacity to effectively resist the coalescence of oil droplets. This is accomplished by increasing the electrostatic repulsion among the charged globules.

3.3 Infrared spectroscopy analysis

The FTIR spectra of LTN, RSV, CMC, and LTN/RSV@CMC are exhibited in Fig. 2d. Luteolin, a flavonoid compound, shows different peaks in its FTIR spectrum (Fig. 2d), notably in the ranges of 3206–3533 cm^{-1} (O–H vibration), 1665 cm^{-1} (C=C vibration), 1340 cm^{-1} (phenolic–OH bending vibration), 1159 cm^{-1} (C–O–C stretching), 1033 cm^{-1}, and 1002 cm^{-1} (C–O–C stretching). This helps to clarify its functional groups and molecular architecture.[52] O–H groups—phenolic and hydroxyl groups—cause the significant absorption band seen in the FTIR spectra of resveratrol at 3200–3500 cm^{-1}. Additional peaks between 1440 and 1590 cm^{-1}, at 1375 cm^{-1}, and at 1145 cm^{-1} point to functional groups in resveratrol, including the benzene ring, aromatic carbon–carbon double bond vibrations, and C–O stretching vibrations.[53] While the peaks at 1010 cm^{-1} and 965 cm^{-1} are related to the bending vibrations of *trans* olefinic C=C, the peak linked with the C–C stretching vibration occurs at 1105 cm^{-1}. Carboxymethyl chitosan (CMC) shows different FTIR peaks at approximately 3400 cm^{-1} (O–H and N–H stretching vibrations), 1600 cm^{-1} (asymmetric stretching of COO^-), 1420 cm^{-1} (symmetric stretching of COO^-), and 1066 cm^{-1} (C–O–C stretching).[54] The peaks point to efficient carboxymethylation and the presence of necessary functional groups in the CMC structure.

FTIR analysis may provide significant insights into the interactions of LTN, RSV, and CMC inside the enclosed system. The amide I band (about 1650 cm^{-1}): variations in this area may signify interactions between the carbonyl groups of LTN/RSV and the amide groups of CMC, implying possible hydrogen bonding or electrostatic interactions. The amide II band (about 1550 cm^{-1}): variations in this band may indicate changes in the secondary structure of CMC after encapsulation. The O–H stretching (about 3200–3500 cm^{-1}) has broad peaks, suggesting the existence of hydrogen bonds associated with the hydroxyl groups of LTN, RSV, and CMC. C–O stretching (about 1000–1200 cm^{-1}): variations in this area may indicate interactions between the carbonyl groups of LTN/RSV and the ether linkages of CMC. Effective encapsulation and probable interactions among the components would be indicated by the observed changes in the FTIR spectra with respect to the individual components.

3.4 XRD pattern of LTN/RSV@CMC

The crystallinity of the compound was indicated by the presence of specific crystalline peaks at 2θ values of 30.3°, 27.5°, 25.5°, 22.9°, 21.5°, 20.4°, 18.5°, 17.2°, 16.3°, 15.9°, 12.8°, and 11.4° in the XRD pattern of pure LTN[55] (Fig. 2e). Conversely, the LTN/RSV@CMC exhibited classic peaks with low intensity at 10°–23°.[56] The observed changes in the height of the peak and intensity serve as confirmation of the solubility of LTN and RSV in the lipids used in the formulation. The pure resveratrol has prominent distinctive peaks at 2θ diffraction angles of 28.7°, 19.1°, and 16.4°, in addition to several minor peaks of diminished strength. The CMC has peaks at 2θ values of 10.5° and 19.2°, suggesting the crystalline structure of the formulated LTN/RSV@CMC nanoemulsion.[57]

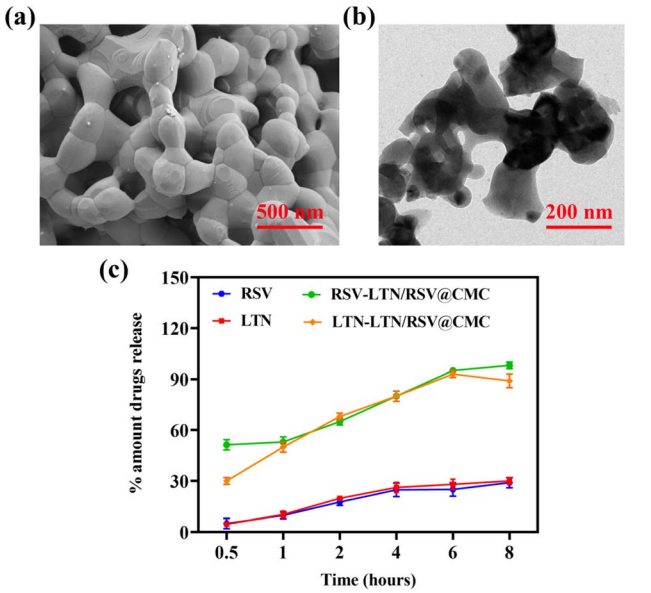

Fig. 3 Morphology of the fabricated LTN/RSV@CMC nanoemulsion. (a and b) SEM and TEM analysis. (c) Release profiles of LTN and RSV from the nanoemulsion.

3.5 Morphological analysis of LTN/RSV@CMC

Fig. 3a and b shows the TEM and SEM images of LTN/RSV@CMC, showing the spherical form with evidence of aggregation for the nanoemulsion droplets. Fig. 3a and b presents the viscosity, pH, and appearance of the LTN/RSV@CMC nanoemulsion. There were no signs of drug precipitation or phase separation; the nanoemulsions seemed homogeneous. With the viscosity measured at 81.23 ± 3.7 mPa s and 6.3 ± 0.0 mPa s, the LTN/RSV@CMC showed lower turbidity.

3.6 *In vitro* drug release/entrapment efficiency (%) studies

This investigation aimed to assess the drug release rates of LTN and RSV from the LTN/RSV@CMC nanoemulsions (Fig. 3c). The examined nanoemulsions greatly improved the release of both medications, producing values much above those of the raw pharmaceuticals. Thirty minutes later, the release percentages of LTN and RSV from the nanoemulsion were 54.1% ± 0.25 and 33% ± 0.4, respectively. Conversely, the associated raw drugs exhibited a release of only 5% ± 1 and 3% ± 0.5 during the same time interval. The raw drugs exhibited only 25% ± 0.15 and 20% ± 0.25, respectively, while the released amounts of LTN and RSV were 97% ± 2.5 and 95% ± 0.2 after 8 hours. The nanoemulsion enhanced release of LTN and RSV is a result of the formulations' small droplet size, which increases the surface area available for drug release. This results in the presence of both drugs in a solubilized micellar solution, which in turn enhances their release from the selected nanoemulsions.[58,59] The Higuchi diffusion model was used to describe the release kinetics of LTN and RSV, which indicated a direct proportional relationship between the quantity of drug released and either the square root of the total drug amount or the drug's solubility in the nanoemulsion formulation.[60] The encapsulation efficiency percentage of the formulated nanoemulsions has been assessed to evaluate the quantities of LTN and RSV incorporated in the oily (internal) phase of LTN/RSV@CMC. The highest encapsulation efficiency percentages were achieved by LTN at 96.75 ± 0.1 and RSV at 97 ± 0.1. This demonstrates a notable enhancement in drug release from the nanoemulsions in comparison to their raw counterparts.

3.7 Biocompatibility and cytotoxicity analysis

First, we evaluated the cytotoxicity on NIH 3T3 cells using CCK-8 assays (Fig. 4) to determine the biocompatibility of LTN/RSV@CMC. Fig. 4a and b shows that about 90% of the cells

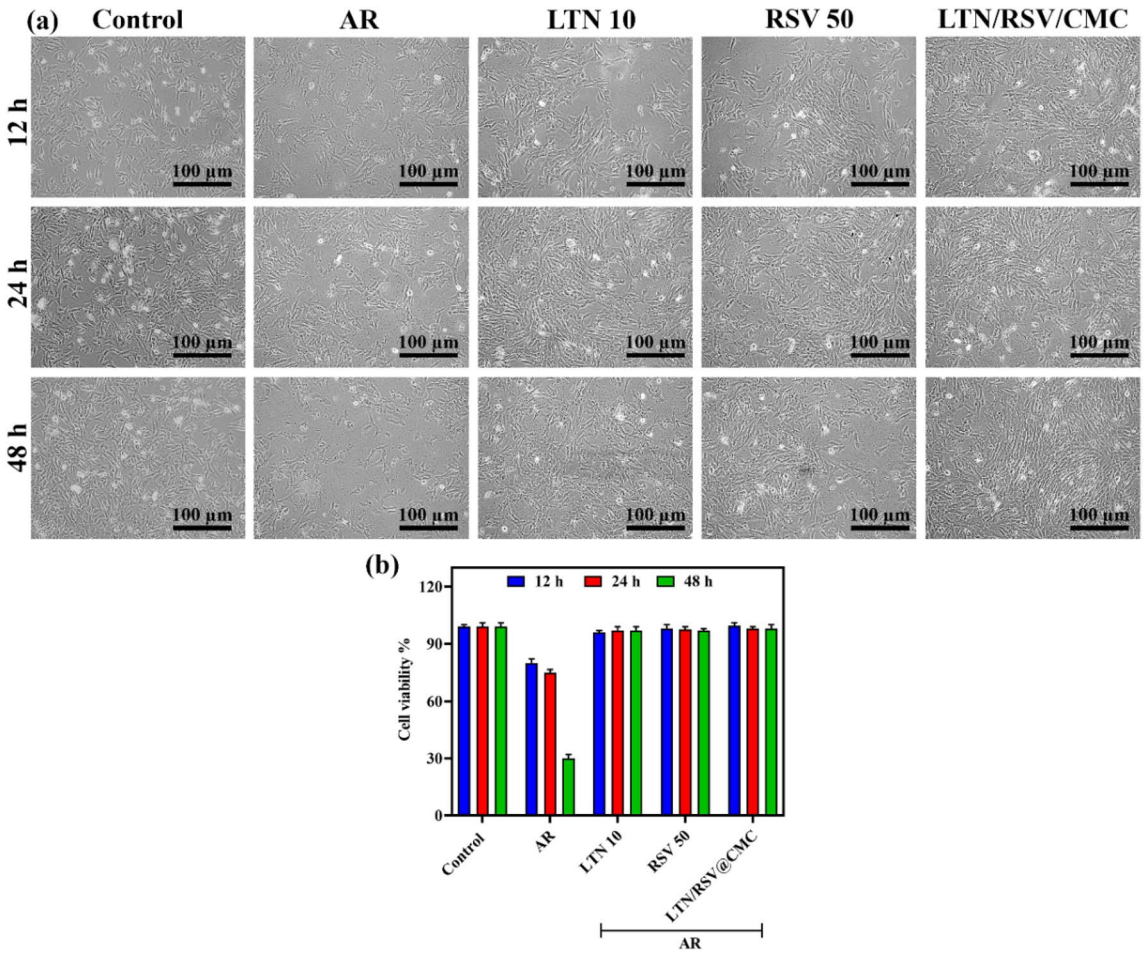

Fig. 4 Biocompatibility of LTN/RSV@CMC nanoemulsion in NIH 3T3 cells. (a) Phase contrast microscopic images of the control, AR, LTN 10, RSV 50 and LTN/RSV@CMC-treated cells. (b) Percentage of cell viability.

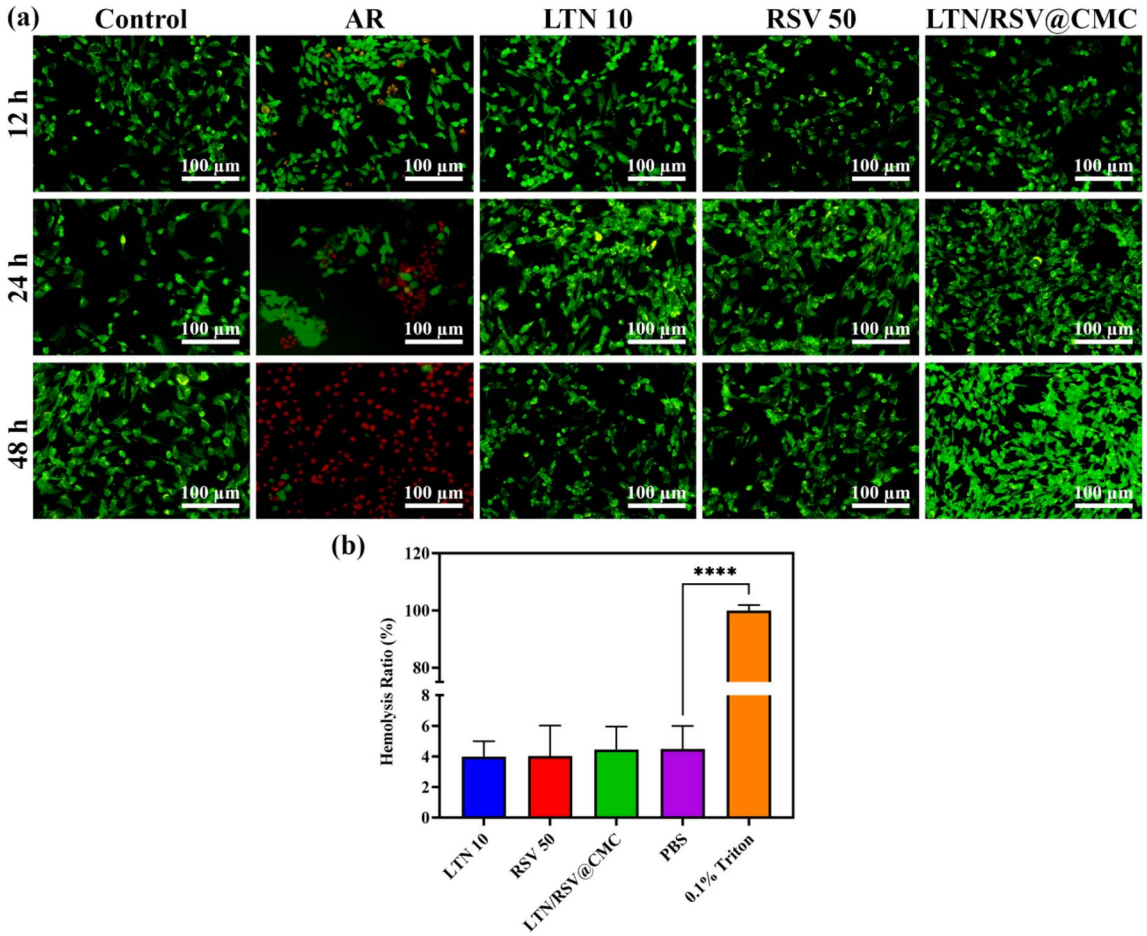

Fig. 5 Biocompatibility of LTN/RSV@CMC. (a) Live/dead staining of the control, AR, LTN 10, RSV 50 and LTN/RSV@CMC in NIH 3T3 cells. (b) Hemolysis rate.

maintained viability after 12, 24, and 48 h across different doses of LTN and RSV, indicating that LTN/RSV@CMC is non-toxic to NIH 3T3 cells. As shown in Fig. 4a and b, the OVA dramatically lowered the cell viability upon 12, 24, and 48 h of treatment.

The live/dead staining provides further evidence of the biocompatibility of LTN/RSV@CMC (Fig. 5a). The LTN and RSV at 10 and 50 mg mL^{-1}, respectively, did not affect the cell viability. We conducted an investigation into the hemolysis rate of LTN/RSV@CMC in light of the possibility for gel penetration into blood vessels during submucosal injection. Fig. 5b illustrates that the hemolysis rate for the LTN/RSV@CMC nano-emulsion stayed below 5%, signifying an absence of significant hemolytic reaction. These results show that the formulated nano-emulsion is biocompatible, which could indicate a promising therapeutic application for AR.

Moreover, in the presence of OVA, the migration and proliferation levels of the LTN/RSV@CMC group were higher than those of the LTN and RSV groups (Fig. 6).

3.8 LTN/RSV@CMC reduced the allergic symptoms

We developed a mouse model of AR through the injection of OVA into the peritoneal cavity of the mice, subsequently followed by the administration of LTN/RSV@CMC.[61] The diagnosis of AR was established when total scores exceeded 5 points.[62] On the 28th day, the mice were observed for approximately 10 minutes following the final nasal challenge, during which their allergic scores were evaluated (Fig. 7a). The AR group showed allergy scores of more than five points. During a 10-minute observation period, the results showed a clear increase in sneezing and nasal rubbing among the AR mice in contrast to the control group, thereby verifying that the OVA injection effectively caused AR symptoms.

The administration of LTN and RSV exhibited an impact in mitigating the AR symptoms. However, mice administered with LTN/RSV@CMC demonstrated a significant decrease in sneezing and nasal rubbing, leading to roughly 60% fewer symptoms in comparison to untreated AR mice (Fig. 7b and c). Although the respective injection of 10 and 50 mg kg^{-1} of LTN and RSV resulted in only moderate decreases in symptoms, the most significant benefits were shown at the combination LTN/RSV dosage, therefore underlining the possible therapeutic value of LTN/RSV@CMC for allergic reactions in this mouse model.

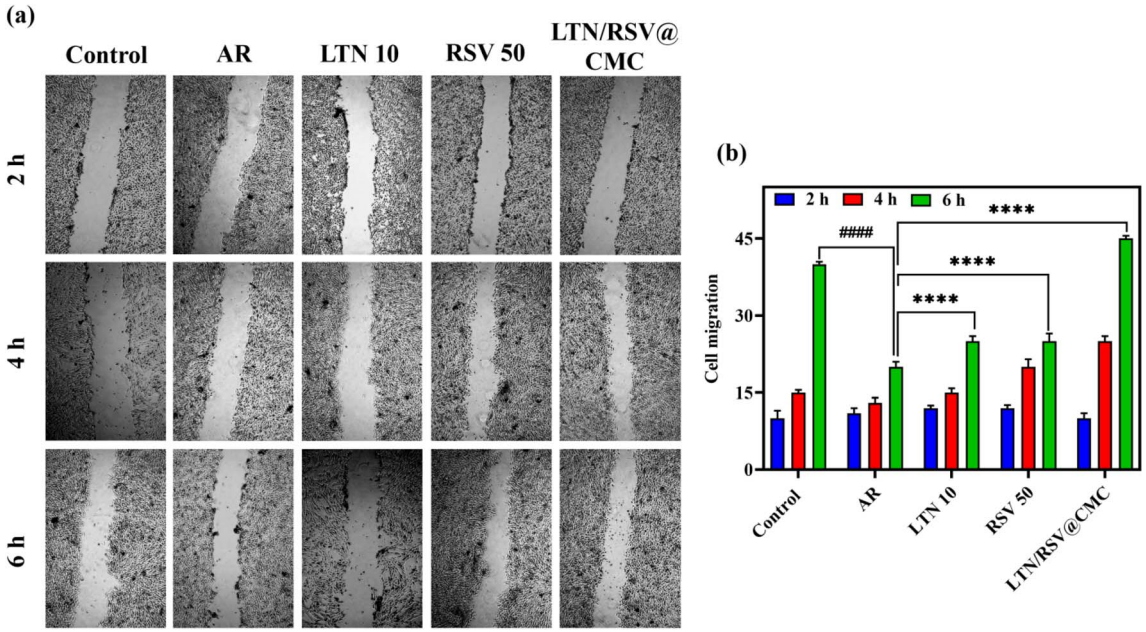

Fig. 6 Cell proliferation analysis of LTN/RSV@CMC-treated NIH 3T3 cells. (a) Cell migration analysis; (b) percentage of cell migration.

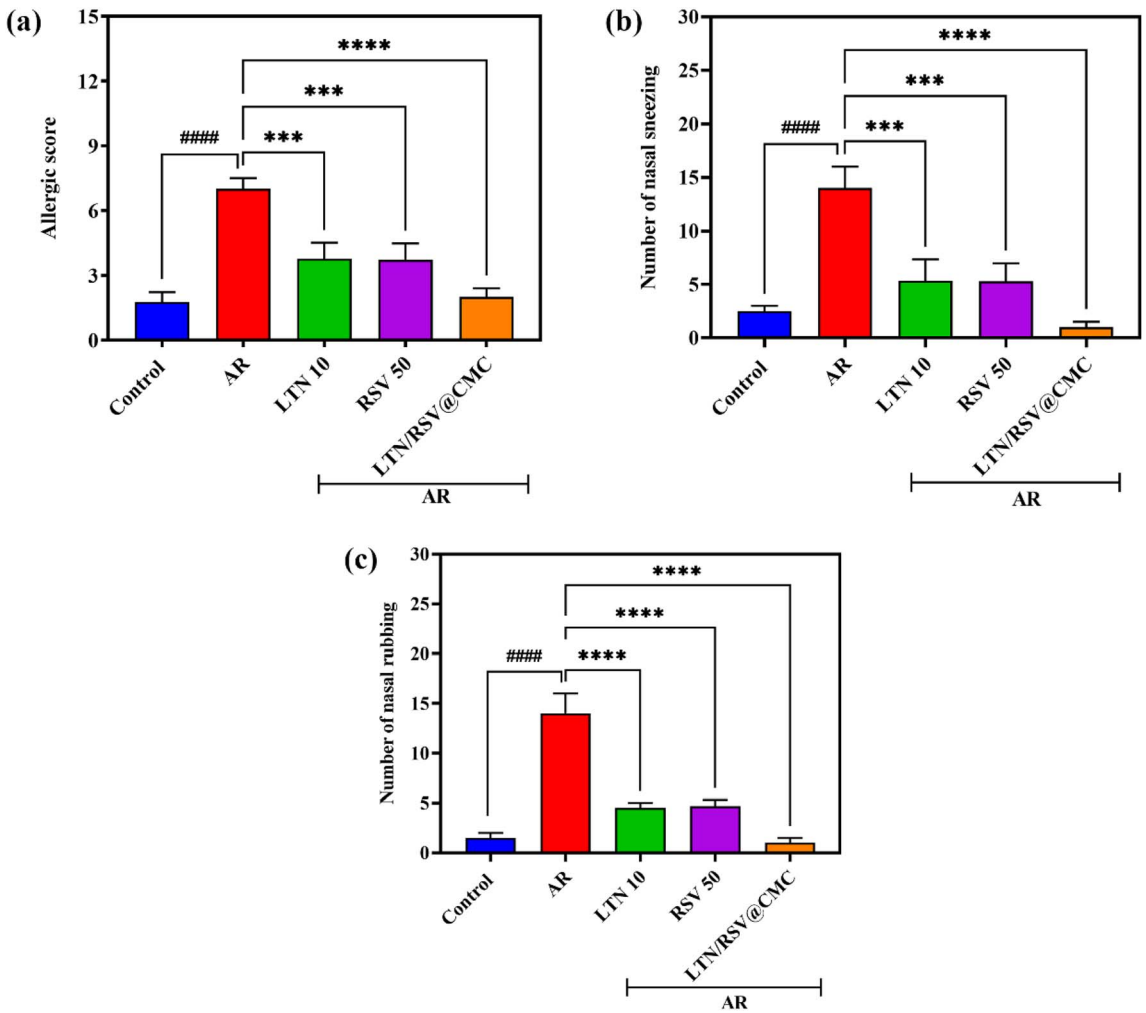

Fig. 7 AR-induced allergic symptoms in the mice model. (a) Allergic score. (b and c) Number of nasal sneezing and rubbing.

3.9 LTN/RSV@CMC reduces the cytokine levels in AR mice

IgE is the initiator and maintainer of allergic diseases, which affect approximately 30% of the global population. Mild manifestations, such as rhinitis, to severe, potentially life-threatening conditions, including asthma and anaphylactic reactions, are all part of the spectrum of symptoms associated with IgE-related allergies.[63] Next, we investigated the possibility that LTN/RSV@CMC could lower serum cytokines in AR mice. AR animals displayed much higher total IgE and OVA-specific IgE than control mice. Treatment with LTN/RSV@CMC clearly reduced serum levels of OVA-specific IgE and IgE of AR mice (Fig. S1a and b). Re-exposure to an allergen activates memory B cells in the sensitizing phase, which then causes them to differentiate into plasma cells. These plasma cells produce rather large amounts of IgE antibodies. High-affinity FcεRI receptors found in mast cells let antibodies bind to them. When allergens contact with the IgE on these cells, a "bridging" reaction results and cellular vesicles are degranulated. Many preformed and recently generated pro-inflammatory mediators produced by this process help to cause an allergic reaction.[63,64] The IL-4 cytokine levels had been considerably higher in AR mice compared to control mice, which suggests the release of pro-inflammatory mediators in response to the AR condition. Following LTN/RSV@CMC treatment, levels of IL-4 also decreased significantly (Fig. S1c). These results indicate that LTN and RSV treatment effectively suppressed IgE levels and IL-4 levels in serum, suggesting that LTN/RSV@CMC reduces AR.

3.10 LTN/RSV@CMC reduces inflammatory cytokine levels

The ability of LTN/RSV@CMC to reduce inflammatory cytokines was further examined. In AR mice, serum levels of the inflammatory cytokines TNF-α, IL-4, -10, -5, -13, -17, exotoxin and IFN-γ (Fig. S2a–h) mRNA were significantly elevated compared to the control mice. Following treatment with LTN/RSV@CMC in AR mice, the levels of these cytokines in serum showed a drastic reduction.

The notable decrease in AR symptoms after treatment with the LTN and RSV suggests a superior therapeutic effect of the LTN/RSV@CMC nanoemulsion. Macrophages release TNF-α in response to external particles, serving as a crucial mediator of the innate immune response. This cytokine induces neighbouring cells to produce interleukin-8 in a paracrine manner, facilitating the recruitment of phagocytes to the inflammatory site.[65] Similarly, IL-5, 10, 13 and 17 levels were measured with ELISA, suggesting that LTN/RSV@CMC significantly reduced the AR-mediated expression of inflammatory cytokines

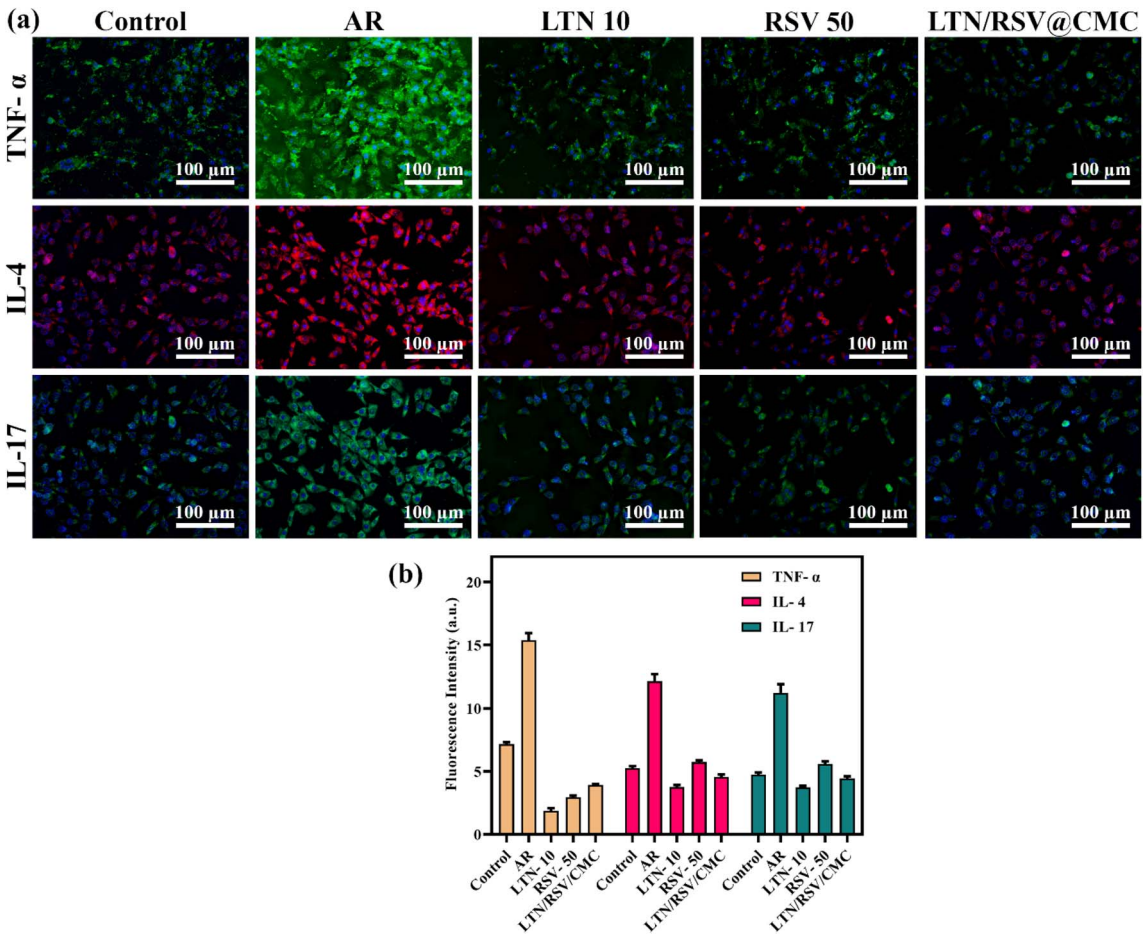

Fig. 8 (a) Immunofluorescence staining of TNF-α (green), IL-4 (red) and 17 (green). (b) Fluorescence intensity. Blue-DAPI.

(Fig. S3a–d). The expressions of TNF-α, IL-4 and 17 were further validated with immunofluorescence staining, which suggest that the nanoemulsion significantly reduced the cytokine levels compared with AR (Fig. 8a and b).

3.11 LTN/RSV@CMC attenuated histamine level in serum and in NLF

Mast cells release histamine and proteases during the effectors phase of allergic reactions, causing local inflammation that results in symptoms like watery nasal discharge, sneezing, and nasal itching.[66] Usually happening in seconds to minutes, the acute hypersensitive reaction passes in a few hours of exposure. By a cooperative mechanism, chemotactic cytokines help immune cells to enter the nasal mucosal tissues.[66,67] Activating invading inflammatory cells produces large amounts of pro-inflammatory mediators and cytokines, including IL-13, -5, -17, -31, and -33. Together, these drugs cause severe inflammatory reactions that cause recurring acute allergy symptoms.[68]

We evaluated the concentrations of histamine in the NLF and serum of AR mice treated with LTN/RSV@CMC, taking into account the critical role of histamine release in the progression of AR. Fig. S4a and b illustrates that AR mice exhibited significantly elevated histamine levels in both NLF and serum in comparison to control mice. However, the LTN/RSV@CMC treatment drastically lowered the amount of histamine in both NLF and serum. The results show that in both NLF and serum of AR mice, LTN/RSV@CMC substantially decreases the levels of histamine.

3.12 LTN/RSV@CMC effectively reduced inflammatory cells in NLF

Interleukins are produced by various immune cell types, such as activated B cells, T cells, monocytes, fibroblasts, and macrophages. As multifunctional cytokines, they are essential in regulating immune responses, participating in the acute-phase reaction, and significantly contributing to the immune response against infections.[69] During the progression of AR, inflammatory cells infiltrate the NLF. To investigate this, we assessed the presence of localized inflammatory cells in the NLF of AR mice and those treated with LTN, RSV and LTN/RSV@CMC. Fig. S5a–d show that the amounts of leukocytes, neutrophils, lymphocytes, and eosinophils in the NLF of AR mice were much higher than those in control mice, which shows that AR has progressed. Notably, LTN/RSV@CMC treatment effectively suppressed the infiltration of leukocytes, neutrophils, lymphocytes, and eosinophils into the NLF. These findings suggest that LTN/RSV@CMC treatment reduces inflammatory cells localized in AR mice. The interleukins regulate the functions of neutrophils and macrophages, thus impacting the immune response. Additionally, they enhance the specificity of the immune response to infected cells and those that present specific foreign antigens by facilitating the differentiation of T and B cells.[70] The results indicate that the AR condition in mice induces pro-inflammatory cytokines, which subsequently infiltrate the immune cells to the NLF.

3.13 Drug toxicity assessment

Mucociliary clearance in the nasal cavity is a vital mechanism of innate immunity that relies on the intricate interaction between three key components: the airway surface fluid layer, mucus layer, and the ciliated epithelium.[71] This study further investigated the impact of LTN/RSV@CMC using *in vivo* histopathology examination. The findings demonstrated a substantial decrease in mast cell and eosinophil numbers inside the nasal mucosa. The alterations noted in the control, AR, LTN 10, RSV 50, and LTN/RSV@CMC groups were in accordance with those depicted in Fig. S6. Furthermore, treatment with LTN/RSV@CMC did not exacerbate nasal mucosa inflammation and exhibited no detrimental effects on nasal epithelial tissues in mice with AR condition. The mucus layer serves as a protective barrier by trapping inhaled particles, pathogens, and allergens, whereas the airway surface fluid layer facilitates the unobstructed and efficient movement of cilia.[71] This dynamic mechanism is crucial in general respiratory health since it helps to keep clear airways and prevents respiratory infections.[72] The mice body weight was tracked throughout the course of treatment. All groups showed a slow rise in body weight, according to the findings and no notable variations were found (Fig. S6b).

4. Conclusion

The LTN/RSV@CMC nanoemulsion can treat allergic responses, according to this investigation on the LTN and RSV loading capacity and therapeutic potential in CMC. The improved formulation increased drug release rates and biocompatibility, as shown by the good cell viability in NIH 3T3 cells and reduced hemolysis. Morphological analyses showed that the nanoemulsion was stable without drug precipitation. In mice, LTN/RSV@CMC reduced sneeze and nasal rubbing relative to untreated controls. The medication also reduced histamine levels and inhibited inflammatory cytokines, suggesting a comprehensive approach to allergy symptom alleviation and inflammation. The findings suggest that nanoemulsions of LTN and RSV may be effective allergen treatments, paving the path for additional research. Because of its biocompatibility, enhanced drug delivery, and significant therapeutic impact, LTN/RSV@CMC is a reasonable allergy treatment choice.

Ethical statement

We have reported this animal investigation in full compliance with the ARRIVE guidelines, thereby guaranteeing transparency and comprehensiveness. All animal procedures were performed in accordance with the Guidelines for the Care and Use of Laboratory Animals of Shaanxi Provincial People's Hospital. The institutional Animal Ethics Committee provided approval for the investigation (approval no. A2024000710).

Author contributions

P. L.: conceptualization, data curation, methodology, validation, visualization, writing – original draft, writing – review &

editing; T. M.: conceptualization, data curation, visualization, writing – review & editing; G. T.: data curation, validation, visualization, writing – review & editing; G. D.: conceptualization, data curation, formal analysis, funding acquisition, investigation, methodology, supervision, validation, writing – original draft, writing – review & editing; K. J.: conceptualization, validation, data curation, visualization, writing – review & editing.

Conflicts of interest

The authors have no competing interests.

Data availability

The datasets generated during the current study are available from the corresponding author upon reasonable request.

Supporting information: OVA specific expression of IgE and pro-inflammatory mediator activation, inflammatory cytokines expression in mRNA level, expression of inflammatory cytokines, histamine level in NLF and serum, infiltration level of inflammatory cells, histopathological analysis of nasal epithelial tissue of mice treated with LTN/RSV@CMC. See DOI: **https://doi.org/10.1039/d5ra03121d**.

References

1 I. C. Camelo-Nunes and D. Solé, *J. Bras. Pneumol.*, 2010, **36**, 124–133.
2 A. Marchetti and R. Rossiter, *J. Med. Econ.*, 2013, **16**, 1399–1404.
3 C. Kogias, A. Drylli, D. Panagiotakos, K. Douros and G. Antonogeorgos, *Allergies*, 2023, **3**, 220–228.
4 P. Liu, C. Kang, J. Zhang, Y. Liu, J. Liu, T. Hu, X. Zeng and S. Qiu, *Int. Immunopharmacol.*, 2022, **113**, 109449.
5 I. Raphael, S. Nalawade, T. N. Eagar and T. G. Forsthuber, *Cytokine*, 2015, **74**, 5–17.
6 C. de Torre-Minguela, P. Mesa del Castillo and P. Pelegrín, *Front. Immunol.*, 2017, **8**, 1–17.
7 Y. Wang, H. Zhao, J. Yang, Z. Cao, L. Hao and Z. Gu, *Food Chem. Toxicol.*, 2024, **184**, 114435.
8 L. Krsmanović, N. Arsović, D. Bokonjić, V. Nešić, Z. Dudvarski, D. Pavlović, M. Dubravac Tanasković, S. Ristić, N. Elez-Burnjaković, R. Balaban, B. Ćurčić, R. Ivanović, N. Vuković, M. Vuković, M. Milić and B. Joksimović, *Biomedicines*, 2024, **12**, 428.
9 A. Ray, K. Gulati, S. Guhathakurta, J. Guhathakurta and N. Rai, *MOJ Immunol.*, 2016, **4**, 00121.
10 M. Minnicozzi, R. T. Sawyer and M. J. Fenton, *Immunol. Rev.*, 2011, **242**, 106–127.
11 K. C. Navegantes, R. de Souza Gomes, P. A. T. Pereira, P. G. Czaikoski, C. H. M. Azevedo and M. C. Monteiro, *J. Transl. Med.*, 2017, **15**, 1–21.
12 R. J. Hewitt and C. M. Lloyd, *Nat. Rev. Immunol.*, 2021, **21**, 347–362.
13 J. Chen, X. Lai, Y. Song and X. Su, *Eur. Respir. Rev.*, 2024, **33**, 240008.
14 R. M. L. Colunga Biancatelli, P. A. Solopov and J. D. Catravas, *Am. J. Pathol.*, 2022, **192**, 837–846.
15 J. G. Souza, N. Starobinas and O. C. M. Ibañez, *Immunology*, 2021, **163**, 377–388.
16 H. Zhou, L. Wang, W. Lv and H. Yu, *Clin. Exp. Med.*, 2024, **24**, 231.
17 M. D. Seidman, R. K. Gurgel, S. Y. Lin, S. R. Schwartz, F. M. Baroody, J. R. Bonner, D. E. Dawson, M. S. Dykewicz, J. M. Hackell, J. K. Han, S. L. Ishman, H. J. Krouse, S. Malekzadeh, J. W. Mims, F. S. Omole, W. D. Reddy, D. V. Wallace, S. A. Walsh, B. E. Warren and M. N. Wilson, *Otolaryngol. – Head Neck Surg.*, 2015, **152**, S1–S43.
18 W. J. Pichler, J. Adam, B. Daubner, T. Gentinetta, M. Keller and D. Yerly, *Med. Clin. North Am.*, 2010, **94**, 645–664.
19 J. Yang, W. Zhong, K. Xue and Z. Wang, *Int. Immunopharmacol.*, 2019, **71**, 76–83.
20 D. Yach, C. Hawkes, C. L. Gould and K. J. Hofman, *JAMA, J. Am. Med. Assoc.*, 2004, **291**, 2616–2622.
21 P. Katare, T. P. Medhe, A. Nadkarni, M. Deshpande, R. K. Tekade, D. Benival and A. Jain, *J. Chem. Health Saf.*, 2024, **31**, 127–143.
22 M. Sadeghi, A. Asadirad, K. Koushki, S. Keshavarz Shahbaz and S. Dehnavi, *Int. Immunopharmacol.*, 2022, **113**, 109327.
23 S. Yuan, T. Ma, Y.-N. Zhang, N. Wang, Z. Baloch and K. Ma, *J. Nanobiotechnol.*, 2023, **21**, 1–25.
24 A. Kumar, A. N. Pandey and S. K. Jain, *Drug Delivery*, 2014, **23**, 671–683.
25 S. Punia Bangar, P. Kajla, V. Chaudhary, N. Sharma and F. Ozogul, *Food Biosci.*, 2023, **52**, 102366.
26 F. Sabatini and I. Degano, *Cultural Heritage Science*, 2022, pp. 247–287.
27 S. Caporali, A. De Stefano, C. Calabrese, A. Giovannelli, M. Pieri, I. Savini, M. Tesauro, S. Bernardini, M. Minieri and A. Terrinoni, *Nutrients*, 2022, **14**, 1155.
28 Y. Han, Y. Xiao, L. Yu, J. Chen, X. Yang, H. Cui and J. Liang, *J. Cancer*, 2023, **14**, 966–980.
29 H. A. Saleh, M. H. Yousef and A. Abdelnaser, *Front. Immunol.*, 2021, **12**, 606069.
30 J. Mlcek, T. Jurikova, S. Skrovankova and J. Sochor, *Molecules*, 2016, **21**, 623.
31 J. Pauluhn and U. Mohr, *Exp. Toxicol. Pathol.*, 2005, **56**, 203–234.
32 C. Liu, Y. He, K. Zhou, H. Wang, M. Zhou, J. Sun, Y. Lu, Y. Huang, Y. Wang, T. Liu and Y. Li, *Heliyon*, 2024, **10**, e37632.
33 Z. Helyes and Z. Hajna, *TRP Channels in Drug Discovery*, 2012, vol. 1, pp. 301–342.
34 Y. Taheri, J. Sharifi-Rad, G. Antika, Y. B. Yılmaz, T. B. Tumer, S. Abuhamdah, S. Chandra, S. Saklani, C. S. Kılıç, S. Sestito, S. D. Daştan, M. Kumar, M. M. Alshehri, S. Rapposelli, N. Cruz-Martins and W. C. Cho, *Oxid. Med. Cell. Longevity*, 2021, **2021**, 1–20.
35 Y. Bellik, L. Boukraâ, H. Alzahrani, B. Bakhotmah, F. Abdellah, S. Hammoudi and M. Iguer-Ouada, *Molecules*, 2012, **18**, 322–353.
36 X. Deng, Y. Wang, L. Jiang, J. Li and Q. Chen, *Front. Immunol.*, 2023, **13**, 1023213.

37 G. Riccioni, M. A. Gammone, G. Tettamanti, S. Bergante, F. R. Pluchinotta and N. D'Orazio, *Int. J. Food Sci. Nutr.*, 2015, **66**, 603–610.
38 A. P. Singh, R. Singh, S. S. Verma, V. Rai, C. H. Kaschula, P. Maiti and S. C. Gupta, *Med. Res. Rev.*, 2019, **39**, 1851–1891.
39 M. Sharifi-Rad, N. V. Anil Kumar, P. Zucca, E. M. Varoni, L. Dini, E. Panzarini, J. Rajkovic, P. V. Tsouh Fokou, E. Azzini, I. Peluso, A. Prakash Mishra, M. Nigam, Y. El Rayess, M. E. Beyrouthy, L. Polito, M. Iriti, N. Martins, M. Martorell, A. O. Docea and W. N. Setzer, *Front. Physiol.*, 2020, **11**, 694.
40 C. B. Williams, The acute impact of a single dose of resveratrol on insulin sensitivity, whole body fat oxidation, and intracellular signaling in skeletal muscle and adipose tissue in overweight and obese men, PhD thesis, Queen's University, Canada, 2013.
41 Y.-F. Zhang, Q.-M. Liu, Y.-Y. Gao, B. Liu, H. Liu, M.-J. Cao, X.-W. Yang and G.-M. Liu, *Food Funct.*, 2019, **10**, 2030–2039.
42 L. O. Lourenço, A. M. Ribeiro, F. D. T. Q. dos Lopes, I. d. F. L. C. Tibério, W. Tavares-de-Lima and C. M. Prado, *Clin. Rev. Allergy Immunol.*, 2021, **62**, 240–263.
43 D. Mu, L. Zhou, L. Shi, T. Liu, Y. Guo, H. Chen, H. Luo, J. Ma, H. Zhang, P. Xiong and L. Tian, *Sci. Rep.*, 2024, **14**, 1–13.
44 S. Thanakkasaranee, K. Jantanasakulwong, Y. Phimolsiripol, N. Leksawasdi, P. Seesuriyachan, T. Chaiyaso, P. Jantrawut, W. Ruksiriwanich, S. R. Sommano, W. Punyodom, A. Reungsang, T. Minh, P. Thipchai, W. Tongdeesoontorn and P. Rachtanapun, *Molecules*, 2021, **26**, 6013.
45 A. Mallick, A. Gupta, A. Hussain, P. Aparajay, S. Singh, S. K. Singh and A. Dev, *J. Drug Delivery Sci. Technol.*, 2020, **56**, 101606.
46 J. C. Byeon, S.-E. Lee, T.-H. Kim, J. B. Ahn, D.-H. Kim, J.-S. Choi and J.-S. Park, *Drug Delivery*, 2019, **26**, 216–225.
47 C. Kilkenny, W. J. Browne, I. C. Cuthill, M. Emerson and D. G. Altman, *PLoS Biol.*, 2010, **8**, e1000412.
48 W. Underwood and R. Anthony, *AVMA Guidelines for the Euthanasia of Animals: 2020 Edition*, 2020.
49 L. Dai, B. Liu, J. Lin, Y. Jiang, Y. Li, Z. Yao, S. Shen, Y. Jiang, Y. Duan and J. Li, *J. Nanobiotechnol.*, 2024, **22**(51), 1–19.
50 Preeti, S. Sambhakar, R. Malik, S. Bhatia, A. Al-Harrasi, C. Indu Rani, R. Saharan, S. Kumar, Geeta and R. Sehrawat, *Scientifica*, 2023, **2023**, 1–25.
51 D. J. McClements, *Curr. Opin. Colloid Interface Sci.*, 2002, **7**, 451–455.
52 S. Rajhard, L. Hladnik, F. A. Vicente, S. Srčič, M. Grilc and B. Likozar, *Processes*, 2021, **9**, 1952.
53 R. Sun, G. Zhao, S. Ni and Q. Xia, *J. Drug Delivery Sci. Technol.*, 2014, **24**, 591–600.
54 H. Zhang, Y. Yi, D. Feng, Y. Wang and S. Qin, *J. Evidence-Based Complementary Altern. Med.*, 2011, **2011**, 691067.
55 K. Xu, B. Liu, Y. Ma, J. Du, G. Li, G. Han, Y. Zhang and Z.-x. Ning, *Molecules*, 2009, **14**, 3486–3493.
56 B. Carletto, J. Berton, T. N. Ferreira, L. F. Dalmolin, K. S. Paludo, R. M. Mainardes, P. V. Farago and G. M. Favero, *Colloids Surf., B*, 2016, **144**, 65–72.
57 P. Moganavally, M. Deepa, P. N. Sudha and R. Suresh, *Orient. J. Chem.*, 2016, **32**, 441–453.
58 S. Alshehri, S. S. Imam, A. Hussain, A. M. Alyousef, M. Altamimi, B. Alsulays and F. Shakeel, *J. Oleo Sci.*, 2020, **69**, 1257–1271.
59 G. Balata, E. Eassa, H. Shamrool, S. Zidan and M. Abdo Rehab, *Drug Des., Dev. Ther.*, 2016, 117.
60 K. Sarpal, Y. B. Pawar and A. K. Bansal, *Curr. Res. Inf. Pharm. Sci.*, 2010, **11**, 42–49.
61 J. Dong, O. Xu, J. Wang, C. Shan and X. Ren, *Immunopharmacol. Immunotoxicol.*, 2021, **43**, 319–327.
62 M. Ozgür Avincsal, S. Ozbal, A. Omer Ikiz, C. Pekcetin and E. Alpin Güneri, *Clin. Exp. Otorhinolaryngol.*, 2014, **7**, 106–111.
63 J. Eckl-Dorna, S. Villazala-Merino, N. J. Campion, M. Byazrova, A. Filatov, D. Kudlay, A. Karsonova, K. Riabova, M. Khaitov, A. Karaulov, V. Niederberger-Leppin and R. Valenta, *Cells*, 2019, **8**, 994.
64 Y. Zhang, F. Lan and L. Zhang, *Allergy*, 2022, **77**, 3309–3319.
65 P.-L. Yao, Y.-C. Lin, C.-H. Wang, Y.-C. Huang, W.-Y. Liao, S.-S. Wang, J. J. W. Chen and P.-C. Yang, *Am. J. Respir. Cell Mol. Biol.*, 2005, **32**, 540–547.
66 A. M. Watts, A. W. Cripps, N. P. West and A. J. Cox, *Front. Pharmacol*, 2019, **10**, 294.
67 S. M. Nur Husna, H.-T. T. Tan, N. Md Shukri, N. S. Mohd Ashari and K. K. Wong, *Front. Med.*, 2022, **9**, 874114.
68 D. Lauritano, F. Mastrangelo, C. D'Ovidio, G. Ronconi, A. Caraffa, C. E. Gallenga, I. Frydas, S. K. Kritas, M. Trimarchi, F. Carinci and P. Conti, *Int. J. Mol. Sci.*, 2023, **24**, 4811.
69 A. A. Al-Qahtani, F. S. Alhamlan and A. A. Al-Qahtani, *Trop. Med. Infect. Dis.*, 2024, **9**, 13.
70 G. Jordakieva and E. Jensen-Jarolim, *World Allergy Organ. J.*, 2018, **11**, 19.
71 X. M. Bustamante-Marin and L. E. Ostrowski, *Cold Spring Harbor Perspect. Biol.*, 2017, **9**, a028241.
72 B. H. Do, T. N. Nguyen, R. Baba, T. Ohbuchi, J.-I. Ohkubo, T. Kitamura, T. Wakasugi, H. Morimoto and H. Suzuki, *Int. Forum Allergy Rhinol.*, 2019, **9**, 1352–1359.